ISSN 1063-7745, Crystallography Reports, 2024, Vol. 69, No. 10, pp. 638–644. © Pleiades Publishing, Inc., 2024.

DIFFRACTION AND SCATTERING OF IONIZING RADIATIONS

Computer Simulation of X-ray Section Topography of Gas Pores in a Silicon Carbide Crystal

V. G. Kohn[a,*]

[a] *National Research Centre "Kurchatov Institute," Moscow, 123182 Russia*

**e-mail: kohnvict@yandex.ru*

Received May 28, 2024; revised July 1, 2024; accepted July 1, 2024

Abstract—The results of computer simulation of images of gas pores in a silicon carbide crystal in section topograms, i.e., during diffraction of a narrow X-ray beam in the crystal, are reported for the first time. The simulation was performed using a special module of the universal computer program XRWP. This program is being developed by the author to calculate the effects of coherent X-ray optics. The calculation method combines two previously known methods, specifically, the Fourier transform method (Kato method) and the method of solving the Takagi–Taupin equations. It is shown that gas pores can produce a wide variety of images, depending on the experimental conditions and the pore position inside the crystal.

DOI: 10.1134/S1063774524601497

INTRODUCTION

X-ray section topography of structure defects in almost perfect crystals is a widely known and efficient method for studying the structure of crystals for microelectronics, primarily, silicon crystals. This method, proposed for the first time in [1], implies that a quasi-monochromatic X-ray beam with a wavelength λ passes through a narrow slit installed before a crystal. Under laboratory conditions the transverse size of a standard source S is relatively large, whereas the distance to the source, z_0, is, in contrast, relatively small, as compared with third-generation synchrotron radiation (SR) sources. For this reason the transverse coherence length $L_{tc} = \lambda z_0/2S$ is very small, and the radiation in the slit is not coherent.

However, as a result of the dynamic diffraction from the crystal lattice, the narrow X-ray beam propagates in the crystal within the Bormann fan (triangle) with an angle of $2\theta_B$ (θ_B is the Bragg angle). This angle may amount to several tens of degrees. In the case of a reflected beam, this fan is filled symmetrically. Correspondingly, the Bormann fan base at a crystal depth t is $2t\sin\theta_B$ in the projection onto the direction perpendicular to the incident beam direction. It may greatly exceed the slit width for a sufficiently thick crystal. Due to this, one can observe interference fringes with a large period (which have a coherent nature) in the crystal image, provided that the slit size is much smaller than this period. In the coherent theory, when the slit is located directly before the crystal, one must perform calculation for all points inside the slit, considering them as independent sources, and then sum the images (intensity) corresponding to all these points. Specifically the peculiarity of the diffraction process, i.e., significant increase in the reflected beam size inside the crystal, makes this experiment almost coherent. If the slit size is small in comparison with the beam size at the crystal output, the summation over the slit size barely changes anything in the central part of the image. The transverse intensity distribution over the slit size is generally averaged in the calculations.

A theoretical calculation of a crystal image obtained by section topography was performed for the first time by Kato in 1961 [2] using a Fourier transform of the wave function of the X-rays incident on the crystal. The sizes of the input X-ray beam were assumed to be infinitely small. The well-known analytical solution to the problem for a plate-like crystal and a plane X-ray wave incident on the crystal was used. In 1962 Takagi [3] proposed a more universal theoretical approach in the form of a system of differential equations for the wave functions of two beams; these equations are simpler than the initial Maxwell equations but take into account in full measure the dynamic effects occurring during X-ray diffraction in single crystals. However, Takagi did not present a solution to these equations. In 1964 Taupin proposed the same equations and then applied them for the first time for numerical calculation of the X-ray diffraction in a crystal containing a dislocation [4].

As a result, the term *Takagi–Taupin equations* became established in the literature. Concerning the Kato method, we will call it the Fourier transform method. A number of works have been published in the next years, where images of single crystals in the

form of a plate containing various structure defects, as well as crystals subjected to external effects, were investigated using methods of numerical solution of the Takagi–Taupin equations. Discussion of those studies and the corresponding references can be found in reviews [5–7].

During growth of some single crystals, gas pores of sufficiently large sizes (more than 10 μm) are formed in their bulk. This fact, paradoxical at first glance, is rather typical; it is observed in various fields of physics and other sciences. Empty sites (vacancies) are collected in one place according to the laws of the elasticity theory. Small water drops on a glass, merging into one large drop, and even people, gathering in huge megacities, behave similarly. Different methods are used to observe gas pores in almost perfect crystals; however, the most efficient technique is apparently the method of X-ray phase-contrast image [8].

At the same time, the standard method of section topography is quite applicable for observing gas pores, for example, in silicon carbide or sapphire. However, there only few such studies in the literature. We should note some recent publications [9, 10], where it is stated (although without any reliable proofs) that the main source of gas pore images in section topograms is the dislocations around pores. Moreover, there are no studies of the theoretical images of gas pores in the crystal bulk, even in the absence of dislocations.

The purpose of this study was to solve this problem for the first time, specifically, to calculate theoretically the images of gas pores in silicon carbide crystals, where they arise rather often. Relatively small pores (smaller than 20 μm) are generally spherically shaped. The complexity of this calculation is in the fact that the lattice inhomogeneity occurs in a small region of the crystal, whereas the crystal itself may be fairly thick. A gas pore must be calculated by the method of Takagi–Taupin equations, which requires a much longer time than the Kato method, which uses the numerical fast Fourier transform [11]. For this reason, we applied for the first time a hybrid approach, combining both aforementioned methods.

The Fourier transform method makes it possible to calculate the two-component wave function of X-rays passing through a perfect crystal to a depth directly before the pore. The pore itself distorts the wave function in a limited region, and this distortion can easily be calculated by the method of Takagi–Taupin equations. Then this distortion must be introduced into the wave function obtained by the Fourier transform method for a perfect crystal at the depth directly behind the pore. After this correction the other part of the crystal can easily be calculated again by the Fourier transform method.

Computer simulation was performed using a modification of the universal computer program XRWP [12], which is based on modular principle of wave optics. This principle implies that the distribution of the wave function in the plane oriented perpendicular to the beam direction is taken into account on a specified computational grid, and this distribution is successively recounted when passing through each object and each distance from one object to another. Having a set of calculation modules for all objects, including empty space, one can perform numerical simulation for any experimental scheme.

In the case under consideration, the crystal was divided into three regions: the defect-free region before the gas pore, the crystal layer containing the pore, and the defect-free region after the pore. Correspondingly, the Fourier transform method was used thrice, and the method of Takagi–Taupin equations was used one time on a limited grid of points. The results obtained unambiguously show that the pore may yield most diverse images, depending on the experimental conditions.

STATEMENT OF THE PROBLEM AND THE METHOD FOR ITS SOLUTION

The main calculation formulas used in the XRWP program were described in [13]. Two-wave diffraction from the atomic lattice in a plate-like crystal occurs in the (x,z) plane; the z axis is chosen to be directed along the normal to the plate surface, and the x axis is parallel to the surface. However, we use another coordinate system for the beams before and after the crystal, in which the z axis is oriented along the beam direction, and the x axis is perpendicular to it. The transition from one system to another is necessary for only the x axis, and it is performed by projecting. In other words, the beam width in air decreases in comparison with the beam width at the crystal input as a result of multiplying by the factor $\cos\theta_B$.

In the case of Laue diffraction in a crystal, instead of one incident beam, we obtain two beams at the crystal output, directed to different sides. Conventionally, the XRWP program "moves" along the trajectory of one beam. In this case, there is always one beam at the input, whereas at the output one should choose one out of two beams for further motion. This is the way in which any of the aforementioned two methods works in the standard experimental scheme. However, calculation in the method of Takagi–Taupin equations is always performed with two beams at the input and at the output. The program uses a modification of the method, which was described in detail in [14]. Calculation is performed in the coordinate system related to the crystal. The Fourier transform method also provides a possibility of working with two beams at the input and at the output. This is necessary for calculating the diffraction in a crystal with a continuation, i.e., with a gradual increase in the crystal thickness. This possibility was used here. The calculation formulas for this method were published in [15]. There is no point in repeating here all the formulas and figures reported in [14, 15].

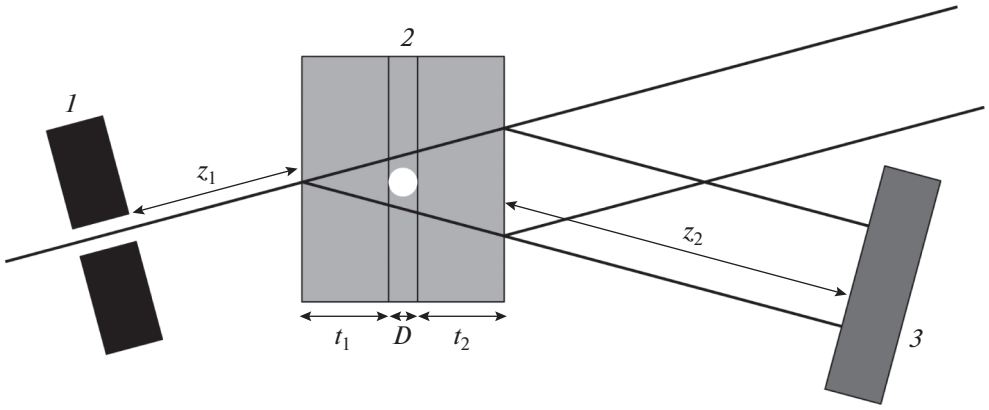

Fig. 1. Schematics of the numerical experiment and illustration of the calculation method: (*1*) slit, (*2*) crystal containing a gas pore, and (*3*) detector. The crystal is divided into three layers: a layer before the pore, a layer containing the pore, and the layer behind the pore.

Figure 1 presents the scheme of the numerical experiment and specific features of the calculation. Although the program can deal with a point source, it is sometimes useful to install a slit of finite thickness before the crystal. As was indicated above, the sizes of the real slit in a laboratory experiment significantly exceed the coherence length, but a slit of smaller size, equal to the coherence length, can be taken into account in the calculation. Sometimes the problem caused by application of the Fourier transform method can be removed in this way. The program can also take into account the distance between the slit and crystal.

The crystal is divided into three layers. The wave functions for the two beams, transmitted and reflected, after the first layer and after the first two layers are calculated by the Fourier transform method fairly rapidly and in a wide region of crystal illumination. Then a part to pass through the pore is selected from the wave function after the first layer. It becomes the input wave function for the method of Takagi–Taupin equations. Since the calculation in this method is performed on a two-dimensional grid of points with different steps along the x and z axes, the calculated wave functions on the x axis must be interpolated to the new grid. To make the program universal, a rectangular region is selected in the crystal, which is characterized by two parameters: width w and height h. This region should completely contain the inhomogeneous part the crystal, in particular, the gas pore.

For the region with these parameters, the range at the output in which changed wave functions are obtained is $w_2 = w + 2h\tan\theta_B$. A calculation by the method of Takagi–Taupin equations makes it possible to obtain a wave function at the output in this range, i.e., at the end of the second layer, if the range $w_1 = w + 4h\tan\theta_B$ is used at the input. This feature of the method is illustrated in Fig. 2. Actually, changes may occur in a smaller region; everything depends on the defect shape. For example, for the cross section of a spherical pore we have $w = h = D$, where D is the diameter of the round cross section. In this case the ranges w_1 and w_2 will be somewhat narrower. This may be useful, because the solutions obtained in two ways can be compared in the regions where they should coincide. Sometimes it is useful to set specially the range w_1 with a margin to make these regions more extended.

The diffraction in a crystal for three-dimensional objects is calculated as a simple set of cross sections. The slit is homogeneous along the y axis. In the crystal, the result is affected by only the change in the cross section of the three-dimensional object by the (x,z) plane with a change in the coordinate y. If there are no such changes, for example, the pore is cylindrical and oriented along the surface, everything remains the same. In the case of spherical pores, changes occur. The center of the round cross section remains where it is, and the diameter D changes. Correspondingly, the thickness t_1 and t_2 for the first and third layers change (Fig. 1). The change in the wave function after the crystal on the distance from the crystal to the detector is two-dimensional if this distance is large. Experimenters generally try to make this distance as small as possible. Here, we consider small distances, on which changes in the image can be neglected. In any case, one must first obtain a two-dimensional array of wave functions on the output crystal surface and then calculate the transmission of radiation in air in three-dimensional space. This is a separate problem.

CALCULATION RESULTS AND THEIR ANALYSIS

A specific calculation was performed for a silicon carbide (SiC) crystal, photon energy $E = 17.479$ keV ($K_{\alpha 1}$ line in the spectrum of the X-ray tube molybde-

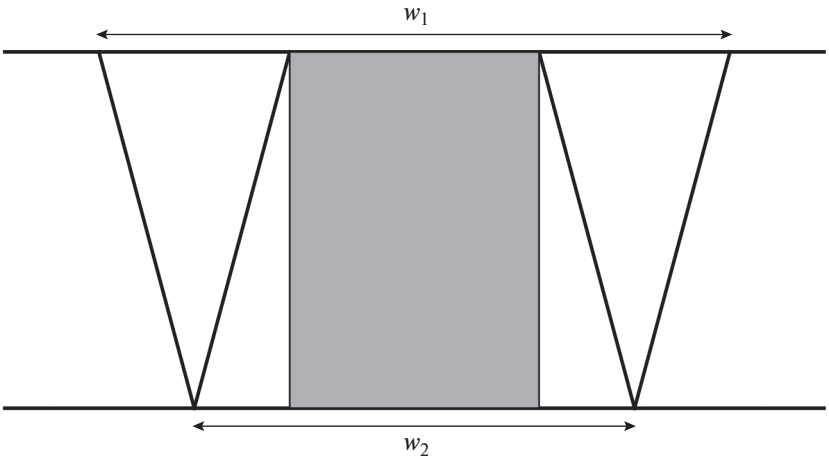

Fig. 2. Crystal layer containing a defect. Each point at the input is a source of perturbations in the Bormann fan with an angle $2\theta_B$ at the vertex. Correspondingly, the rectangular region distorts the wave function of the beams at the output in the range w_2. To perform a correct calculation in this range by the method of Takagi–Taupin equations, one must know the wave functions in the range w_1.

num anode), and the 220 reflection. The diffraction parameters were calculated using the on-line-program [16] to be

$$\begin{aligned} K\chi_0 &= -0.3872 + 0.001431i, \\ K\chi_h &= -0.19682 + 0.001407i, \\ \theta_B &= 13.303°. \end{aligned} \quad (1)$$

Here, $K = 2\pi/\lambda$ is the wave number. The section topogram of a perfect crystal is known well (see textbooks [17, 18]). The intensity of an infinitely narrow beam is distributed in the Bormann fan; at relatively small thicknesses, Kato interference fringes, inscribed in this fan, are formed. In this case, the wave function at a specified crystal thickness is the crystal propagator in the sense that the problem of the transmission of arbitrary radiation through the crystal is solved by calculating the convolution of the wave function on the input surface and the crystal propagator [19].

The crystal propagator is known to be described by a Bessel function of a complex argument, which depends in a complicated way on the coordinate x and crystal thickness t. In the presence of a coherent slit located at some distance from the crystal, the Bessel function is distorted, and the exact value is calculated by the program. At a small slit size and a small distance, the distortion is also small. Figure 3 shows the change in the radiation intensity with an increase in the crystal thickness t for the aforementioned parameters along the normal to the surface from the Bormann fan vertex, obtained using the program for the slit width $S_1 = 1$ μm and the distance between the slit and crystal $z_1 = 5$ cm. The oscillation period is maximum along this line.

The I_0 value in the figure is chosen such as to make the second and next maxima be seen well. The first maximum is cut in these units; in reality, it is larger by a factor of 6. If we assume the radiation intensity before the slit be unity, $I_0 = 0.01$. It is known that the crystal propagator is unity at $t = 0$, after which it decreases. If $z_1 > 0$ and the slit is wide, the effect of diffraction focusing occurs [20], at which the maximum shifts into the crystal bulk. In the case under consideration, this microdisplacement occurs as well.

Figure 4 shows four section topograms, calculated using the developed program for a spherical gas pore with a diameter $D = 18$ μm and the center located on the line in Fig. 3. The calculation parameters (Fig. 1) are as follows: $z_1 = 5$ cm; $t_1 = 319$ μm; $t_2 = 0$, 20, 100, 200 μm; and $z_2 = 0$. Here, only the thickness of the second layer of the perfect crystal (i.e., after the defect) changes. The order is obvious: from top to bottom. As follows from Fig. 3, the first layer ends in the region of maximum oscillating radiation intensity. The beginning of the second layer is in the region of minimum. In the upper fragment the gas pore looks bright against a dark background. It simply transfers radiation from the upper to lower layer almost without distortions (small distortions are nevertheless present).

The situation changes with an increase in the thickness of the second layer, t_2. In this layer the defect becomes a source of distortions of the standard pattern, which propagate again in a Bormann fan with the vertex located near the defect. The perturbation region expands horizontally (along the x axis) with an increase in the thickness t_2, while changes in the vertical direction (along the y axis) occur within the spherical pore diameter. The brightest pore image is nevertheless transferred in the directions of the reflected

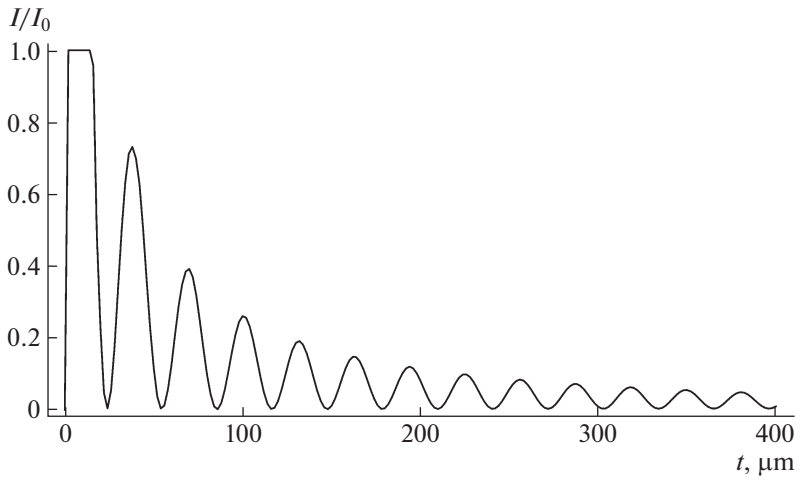

Fig. 3. Dependence of the relative intensity on the crystal thickness along the central line in a section topogram. The first maximum is cut off; in reality, it is higher by a factor of 6.

(on the left) and transmitted (on the right) beams. As well as in the method of X-ray phase-contrast image, different parts of the sphere differently perturb the wave function. In this case, the crystal thickness plays the role of distance in empty space in the method of phase-contrast image, which makes it possible to show changes in the wave function phase. An effect similar to focusing occurs in some regions.

In the upper fragment the Bormann fan base, projected onto the reflected-beam cross section, is $2t\sin\theta_B$ = 155 μm; i.e., is smaller than the image size. A maximum is obtained on the oscillation second from the edge rather than on the extreme one, as in the crystal propagator. This occurs because of the finiteness of the slit size and the distance z_1. The range of illumination of other crystal fragments is wider than shown in the plot. In each fragment the contrast is shown from zero to the maximum value, which is arbitrarily assumed to be unity in the plot. The real values of the relative intensity maximum are different in different fragments. On the assumption that the relative intensity before the slit is unity, these values are 1.76×10^{-3}, 1.86×10^{-3}, 1.11×10^{-3}, and 0.82×10^{-3}.

Calculation of topograms in Fig. 4 was also performed for $z_1 = 0$ to find out how a small distance affects the character of images. The differences turned out to be too small to detect. For this reason it makes no sense to take into account the short distance after the crystal as well. This is what has usually been done for the last 50 years when calculating section topograms for comparison with the results of laboratory measurements. When using SR sources, the wave function after the crystal can be transferred using different devices, for example, refractive lenses. However, such experiments have not been performed yet.

Figure 5 shows the topograms calculated with the same parameters as in Fig. 4, except for the one: t_1 = 303 μm. As follows from Fig. 3, the first layer ends in the region of minimum intensity in this case. For this reason the image in the upper fragment is inverted: pores are black against the bright background. A certain regularity can be noted at other distances: the pore

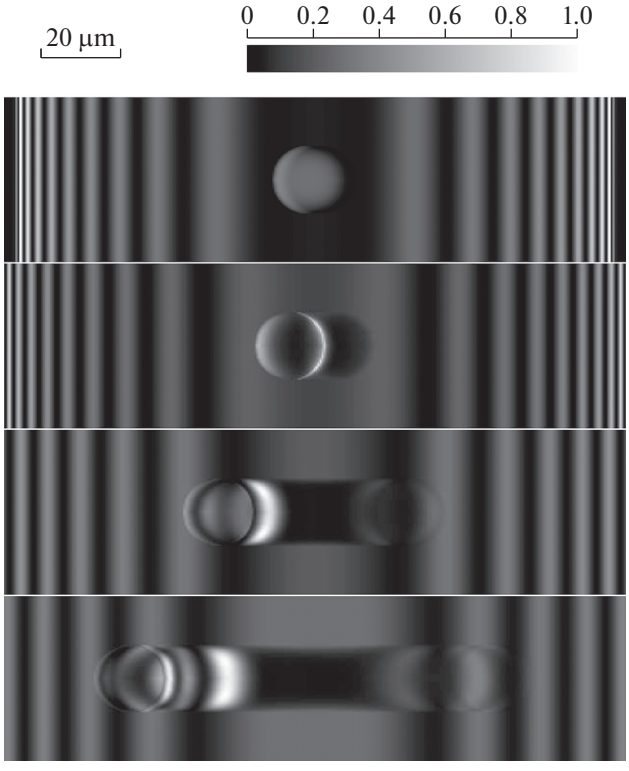

Fig. 4. Series of four section topograms, calculated with the following parameters: photon energy E = 17.479 keV; slit width S_1 = 1 μm; z_1 = 5 cm; t_1 = 319 μm; t_2 = 0, 20, 100, 200 μm; z_2 = 0; and D = 18 μm. The order of variation in t_2 is from top to bottom.

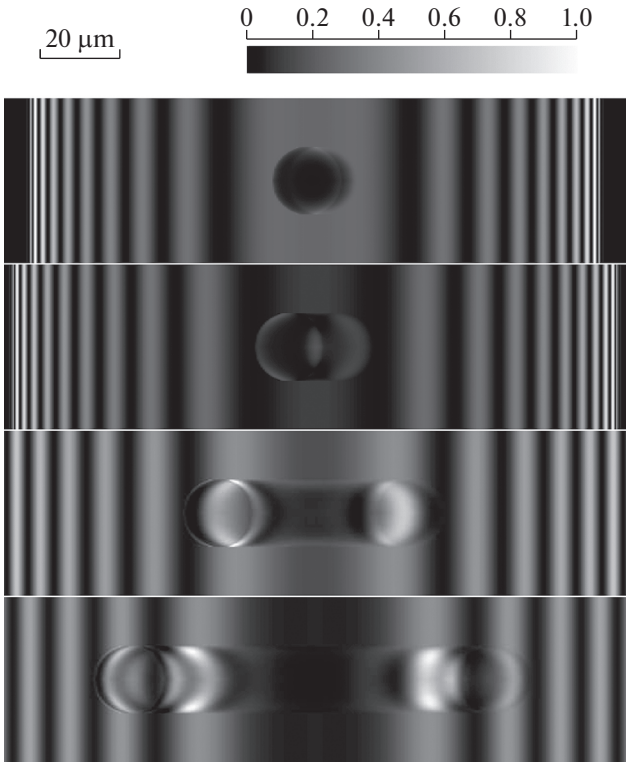

Fig. 5. Series of four section topograms, calculated with the same parameters as in Fig. 4, except for t_1: 303 μm. The order of variation in t_2 is from top to bottom.

image correlates with that of the perfect crystal. The pore is bright in the region where bright bands were observed and dark in the region containing previously dark bands. At the same time, the images are more symmetric: the patterns on the left and on the right are almost the same.

CONCLUSIONS

A new method was developed to calculate lattice defects with limited sizes in section topograms. The calculation results for a spherical pore 18 μm in diameter showed that gas pores can yield most diverse images, depending on the pore position in the crystal. To understand in detail the principles of image formation, it is necessary to perform a large series of calculations. What is clear now is only that pore images can be obtained in section topograms, but very narrow slits must be used to this end. With a slit 10 μm in size or larger, images can be significantly averaged and difficult to distinguish. In principle, a beam focused by a refractive lens can be used instead of slits [21]. However, one must bear in mind that the angular range of a refractive lens greatly exceeds the angular range of diffraction in crystals; therefore, there will be no gain in intensity.

In addition, it is necessary to understand how the emission spectrum in combination with the wide angular range of the lens affects the images in section topograms. The spectrum in SR sources must be limited using a monochromator. Laboratory measurements of angular dependences are generally performed using double-crystal nondispersive schemes, but in the section topography the entire spectrum of characteristic radiation is taken into account, which makes the slit an incoherent source to a greater extent. The analysis of these questions is beyond the scope of this study, but it may be carried out in future.

FUNDING

This study was performed within the State assignment for the National Research Centre "Kurchatov Institute."

CONFLICT OF INTEREST

The author of this work declares that he has no conflicts of interest.

REFERENCES

1. N. Kato and A. R. Lang, Acta Crystallogr. **12**, 787 (1959). https://doi.org/10.1107/S0365110X61001625
2. N. Kato, Acta Crystallogr. **14**, 627 (1961). https://doi.org/10.1107/S0365110X61001947
3. S. Takagi, Acta Crystallogr. **15**, 1611 (1962). https://doi.org/10.1107/S0365110X62003473
4. D. Taupin, Acta Crystallogr. **23**, 25 (1967). https://doi.org/10.1107/S0365110X67002063
5. J. Gronkowski, Phys. Rep. **206**, 1 (1991). https://doi.org/10.1016/0370-1573(91)90086-2
6. E. V. Suvorov and I. A. Smirnova, Phys.-Usp. **58**, 833 (2015). https://doi.org/10.3367/UFNe.0185.201509a.0897
7. I. L. Shul'pina, E. V. Suvorov, I. A. Smirnova, et al., Tech. Phys. **67**, 1277 (2022). https://doi.org/10.21883/TP.2022.10.53354.23-22
8. T. S. Argunova and V. G. Kohn, Phys.-Usp **62**, 602 (2019). https://doi.org/10.3367/UFNe.2018.06.038371
9. T. S. Argunova, V. G. Kohn, J.-H. Lim, et al., Materials (MDPI) **16**, 6589 (2023). https://doi.org/10.3390/ma16196589
10. T. S. Argunova, V. G. Kohn, J.-H. Lim, et al., J. Surf. Invest.: X-ray, Synchrotron Neutron Tech. **17** (Suppl. 1), S20 (2023). https://doi.org/10.1134/S1027451023070030
11. J. W. Cooley and J. W. Tukey, Math. Comput. **19**, 297 (1965).
12. V. G. Kohn, XRWP program. http://xray-optics.ucoz.ru/XR/xrwp.htm
13. V. G. Kohn, http://xray-optics.ucoz.ru/XR/xrwp-equations.pdf

14. V. G. Kohn, Crystallogr. Rep. **68**, 210 (2023). https://doi.org/10.1134/S1063774523020086
15. V. G. Kohn and I. A. Smirnova, Crystallogr. Rep. **66**, 897 (2021). https://doi.org/10.1134/S1063774521060195
16. V. G. Kohn, On-line program https://kohn-vict.ucoz.ru/jsp/3-difpar.htm.
17. A. Authier, *Dynamical Theory of X-ray Diffraction* (Oxford Univ. Press, New York, 2005).
18. Z. G. Pinsker, *Dynamical Scattering of X-Rays in Crystals* (Springer, 1978).
19. A. M. Afanasev and V. G. Kohn, Acta Crystallogr. A **27**, 421 (1971).
20. A. M. Afanas'ev and V. G. Kohn, Fiz. Tverd. Tela **19**, 1775 (1977).
21. A. Snigirev, V. Kohn, I. Snigireva, et al., Nature **384**, 49 (1996).

Translated by Yu. Sin'kov